

This is a repository copy of *The Human Posterior Superior Temporal Sulcus Samples Visual Space Differently From Other Face-Selective Regions*.

White Rose Research Online URL for this paper:

<https://eprints.whiterose.ac.uk/148493/>

Version: Accepted Version

---

**Article:**

Pitcher, David James, Pilkington, Amy, Rauth, Lionel et al. (3 more authors) (2019) The Human Posterior Superior Temporal Sulcus Samples Visual Space Differently From Other Face-Selective Regions. *Cerebral Cortex*. pp. 778-785. ISSN 1460-2199

<https://doi.org/10.1093/cercor/bhz125>

---

**Reuse**

Items deposited in White Rose Research Online are protected by copyright, with all rights reserved unless indicated otherwise. They may be downloaded and/or printed for private study, or other acts as permitted by national copyright laws. The publisher or other rights holders may allow further reproduction and re-use of the full text version. This is indicated by the licence information on the White Rose Research Online record for the item.

**Takedown**

If you consider content in White Rose Research Online to be in breach of UK law, please notify us by emailing [eprints@whiterose.ac.uk](mailto:eprints@whiterose.ac.uk) including the URL of the record and the reason for the withdrawal request.

**The human posterior superior temporal sulcus (pSTS)  
samples visual space differently from other face-selective regions**

David Pitcher <sup>1</sup>, Amy Pilkington <sup>1</sup>, Lionel Rauth <sup>2</sup>, Chris Baker <sup>3</sup>, Dwight J Kravitz <sup>4</sup>  
& Leslie G Ungerleider <sup>2</sup>

1. Department of Psychology, University of York, Heslington, York, YO105DD, U.K.
2. Section on Neurocircuitry, Laboratory of Brain and Cognition, National Institute of Mental Health, Bethesda, MD, 20892, U.S.A.
3. Section on Learning and Plasticity, Laboratory of Brain and Cognition, National Institute of Mental Health, Bethesda, MD, 20892, U.S.A.
4. Department of Psychology, George Washington University, 2125 G Street NW, Washington, DC, 20052, U.S.A.

Corresponding author: David Pitcher - Email: david.pitcher@york.ac.uk

Department of Psychology, University of York, Heslington, York, YO105DD, U.K.

**Keywords**

Face processing, fusiform face area (FFA), occipital face area (OFA), Amygdala

## **Abstract**

Neuroimaging studies show that ventral face-selective regions, including the fusiform face area (FFA) and occipital face area (OFA), preferentially respond to faces presented in the contralateral visual field (VF). In the current study we measured the VF response of the face-selective posterior superior temporal sulcus (pSTS). Across three functional magnetic resonance imaging (fMRI) experiments, participants viewed face videos presented in different parts of the visual field. Consistent with prior results, we observed a contralateral VF bias in bilateral FFA, right OFA (rOFA) and bilateral human motion-selective area MT+. Intriguingly, this contralateral VF bias was absent in the bilateral pSTS. We then delivered transcranial magnetic stimulation (TMS) over right pSTS (rpSTS) and rOFA, while participants matched facial expression in both hemifields. TMS delivered over the rpSTS disrupted performance in both hemifields, but TMS delivered over the rOFA disrupted performance in the contralateral hemifield only. These converging results demonstrate that the contralateral bias for faces observed in ventral face-selective areas is absent in the pSTS. This difference in VF response is consistent with face processing models proposing two functionally distinct pathways. It further suggests that these models should account for differences in interhemispheric connections between the face-selective areas across these two pathways.

## **Introduction**

Neuroimaging studies have identified multiple face-selective areas across the human brain. These include the fusiform face area (Kanwisher et al., 1997; McCarthy et al., 1997), occipital face area (Gautier et al., 2000) and posterior superior temporal sulcus (Puce et al., 1997; Phillips et al., 1997). Models of face perception (Haxby et al., 2000; Calder & Young, 2005) propose that these areas are components in two separate and functionally distinct neural pathways: a ventral pathway specialized for recognising facial identity (that includes the FFA), and a lateral pathway specialized for recognising facial expression (that includes the pSTS). While these pathways perform different cognitive functions, both are thought to begin in the OFA, the most posterior face-selective area in the human brain. Alternative models have proposed different cortico-cortical connections for the face-selective pSTS. One theory proposes that the pSTS has anatomical and functional connections with the motion-selective area human MT+ (hMT+), which are independent of the OFA (O'Toole et al., 2002; Gschwind et al., 2012; Pitcher et al., 2014, Yovel & Duchaine, 2015). In the current study, we sought to further investigate the functional connections of the pSTS using functional magnetic resonance imaging (fMRI) and transcranial magnetic stimulation (TMS).

Our recent neuropsychological and combined TMS / fMRI studies suggest that the rpSTS is functionally connected to brain areas other than the rOFA and rFFA (Reslezcu et al., 2012; Pitcher et al., 2014). These studies demonstrated that disruption of the rFFA and rOFA did not reduce the neural response to moving faces in the rpSTS, suggesting it is functionally connected to other brain areas. However, these studies did not

investigate which brain areas may be functionally connected with the rpSTS. As suggested previously, hMT+ may have functional connections with the rpSTS (O'Toole, 2002) but alternate potential candidate areas are also plausible, notably face-selective areas in the contralateral hemisphere. For example, a recent study demonstrated that TMS delivered over the rpSTS and lpSTS impaired a facial expression recognition task (Sliwiska & Pitcher, 2018). This suggests that face-selective areas in both hemispheres are necessary for optimal task performance.

In the present study, we investigated the visual field responses to faces in face- and motion-selective areas to better understand the functional connections of the rpSTS. Prior evidence has shown that the FFA and OFA exhibit a greater response to faces presented in the contralateral compared to the ipsilateral visual field (Hemond et al., 2007; Chan et al., 2010; Kay et al., 2015). However, the visual field responses to faces in the posterior superior temporal sulcus (pSTS) has not been established. If, like the FFA and OFA, the pSTS shows a greater response to faces presented in the contralateral visual field this would suggest that the dominant functional inputs to the pSTS come from brain areas in the ipsilateral hemisphere. If, however, the pSTS responds to faces in the ipsilateral visual field to a greater extent than the FFA and OFA, then the pSTS is likely to have greater functional connectivity with the contralateral hemisphere.

We used fMRI to measure the neural response evoked by short videos of faces presented in the four quadrants of the visual field in face-selective areas (Experiment 1) and in hMT+ (Experiment 2). In Experiment 3, we increased the size of the stimulus videos and presented them in the two visual hemifields. This was done to increase the

size of the neural responses across face-selective regions. Finally, in Experiment 4, we used transcranial magnetic stimulation (TMS) to investigate if visual field responses were reflected in behaviour. TMS was delivered over the rOFA, rpSTS or the vertex control site while participants performed a behavioural facial expression recognition task in the two visual hemifields. Our results were consistent across all experiments; namely, the bilateral FFA (FFA), rOFA, and bilateral hMT+ all exhibited a greater response to faces presented in the contralateral than ipsilateral visual field (we were unable to functionally identify the left OFA in a sufficient number of participants). By contrast, the bilateral pSTS showed no preference for faces presented in any part of the visual field. This same pattern was observed in Experiment 4: TMS delivered over the rpSTS disrupted task performance in both hemifields, but TMS delivered over the rOFA disrupted performance in the contralateral hemifield only. Our results demonstrate a functional difference in the interhemispheric connectivity between face-selective areas on the ventral and lateral brain surfaces.

## **Materials and Methods**

### **Participants**

In Experiments 1-3, a total of 23 right-handed participants (13 females, 10 males) with normal, or corrected-to-normal, vision gave informed consent as directed by the National Institutes of Mental Health (NIMH) Institutional Review Board (IRB). Eighteen participants were tested in Experiment 1, thirteen in Experiment 2, and eighteen in Experiment 3. Thirteen of the participants took part in all the fMRI experiments (1-3). In

Experiment 4, fourteen right-handed participants (8 females, 6 males) with normal, or corrected-to-normal, vision gave informed consent as directed by the Ethics committee at the University of York.

## **Stimuli**

### Regions-of-interest (ROIs) Localizer Stimuli

In Experiments 1, 3 and 4, face-selective regions-of-interest (ROIs) were identified using 3-sec video clips of faces and objects. These videos were used in previous fMRI studies of face perception (Pitcher et al., 2011; 2014; 2017). Videos of faces were filmed on a black background and framed close-up to reveal only the faces of 7 children as they danced or played with toys or with adults (who were out of frame). Fifteen different moving objects were selected that minimized any suggestion of animacy of the object itself or of a hidden actor moving the object. Stimuli were presented in categorical blocks and, within each block, were randomly selected from the entire set for that stimulus category. This meant that the same actor or object could appear within the same block. The order of repeats was randomized and happened on average once per block. Participants were instructed to watch the movies and to detect when the subject of the video was repeated (one-back task). Repeats occurred randomly at least two times per run.

In Experiment 2, hMT+ was identified using a motion localizer. This localizer used an on/off block design to identify parts of the brain that respond more strongly to coherent dot motion than random dot motion. Stimuli were presented in 12 alternating blocks of

coherent and random motion (11.43 sec each). In both conditions, 150 white dots (dot diameter: 0.04 degrees, speed: 5.0 degrees/sec) appeared in a circular aperture (diameter: 9 degrees). During blocks of coherent motion, dots changed their coherent direction every sec to avoid adaptation to any maintained direction of motion. The dots in the incoherent condition changed every second but the changes were not coordinated with each other to generate the appearance of random motion. Participants were instructed to focus on a red fixation dot presented at the center of the screen. HMT+ was identified using a contrast of activation evoked by coherent dot motion greater than that evoked by random dot motion (noise).

#### fMRI Face Visual Field Mapping Stimuli (Experiments 1-3)

Visual field responses in face-selective regions were mapped using 2-sec video clips of dynamic faces making one of four different facial expressions: happy, fear, disgust and neutral air-puff. These faces were used in a previous fMRI study of face perception (van der Gaag et al., 2007). Happy expressions were recorded when actors laughed spontaneously at jokes, whereas the fearful and disgusted expressions were posed by the actors. The neutral, air-puff condition consisted of the actors blowing out their cheeks to produce movement but expressing no emotion. Both male and female actors were used. Videos were filmed against a gray background and the actors limited their head movements. In Experiments 1 and 2, videos were presented at 3 by 3 degrees of visual angle and were shown centered in the four quadrants of the visual field at a distance of 5 degrees from fixation to the edge of the stimulus (Kravitz et al., 2010).



Experiment 3 followed the same procedure as Experiments 1 and 2, except that faces were presented in the contralateral and ipsilateral visual hemifields (see Figure 1). Videos were presented at 5 by 5 degrees of visual angle and shown at a distance of 5 degrees from fixation to the edge of the stimulus. The size of the videos was increased in order to increase the neural response recorded in face-selective areas.

**Figure 1 Here.**

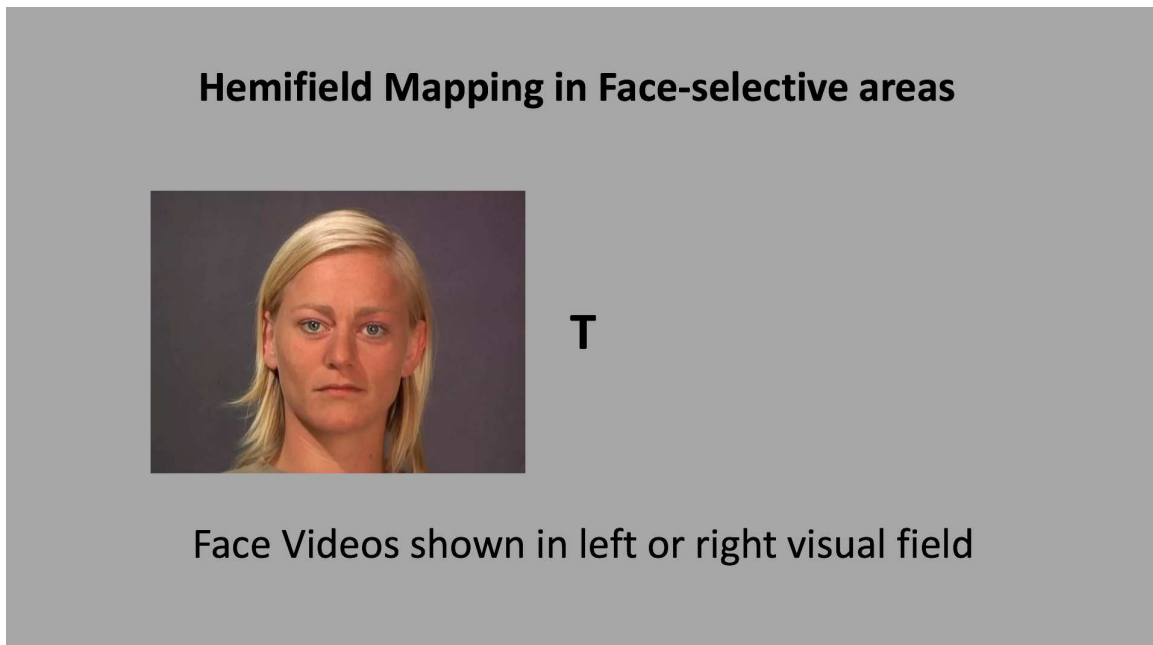


Figure 1. Static image taken from the hemifield visual field mapping stimulus used in Experiment 3. Actors displaying different emotions (happy, fear, disgust, neutral air-puff) were shown in the two hemifields of the visual field. Participants maintained fixation by detecting the presence of either a T or an L (shown upright or inverted) at fixation and were informed of their performance at the end of each block. Runs in which the participant failed to perform the task at an accuracy of seventy-five percent correct were excluded from further analysis.

### TMS Face Visual Field Mapping Stimuli (Experiment 4)

Face stimuli were six female models (C, MF, MO, NR, PF and SW) from Ekman and Friesen's (1976) facial affect series expressing one of six emotions: happy, sad, surprise, fear, disgust and anger. Each grayscale picture was cropped with the same contour using Adobe Photoshop to cover the hair, ears and neck.

### **Procedure**

#### **Brain Imaging Acquisition and Analysis**

Participants were scanned using research dedicated GE 3-Tesla scanners at the National Institutes of Health (NIH) (Experiments 1-3) and the University of York (Experiment 4). In Experiments 1 and 2, whole brain images were acquired using an 8-channel head coil (36 slices,  $3 \times 3 \times 3$  mm, 0.6 mm interslice gap, TR = 2 sec, TE = 30 msec). In Experiment 3, whole brain images were acquired using a 32-channel head coil (36 slices,  $3 \times 3 \times 3$  mm, 0.6 mm interslice gap, TR = 2 sec, TE = 30 msec). In Experiment 4, whole brain images were acquired using a 12-channel head coil (32 slices,  $3 \times 3 \times 3$  mm, 0.6 mm interslice gap, TR = 3 sec, TE = 30 msec). Slices were aligned with the anterior/posterior commissures. In addition, a high-resolution T-1 weighted MPAGE anatomical scan (T1-weighted FLASH, 1 x 1 x 1 mm resolution) was acquired to anatomically localize functional activations.

Functional MRI data were analyzed using AFNI (<http://afni.nimh.nih.gov/afni>). Data from the first four TRs from each run were discarded. The remaining images were slice-

time corrected and realigned to the third volume of the first functional run and to the corresponding anatomical scan. The volume-registered data were spatially smoothed with a 5-mm full-width-half-maximum Gaussian kernel. Signal intensity was normalized to the mean signal value within each run and multiplied by 100 so that the data represented percent signal change from the mean signal value before analysis.

A general linear model (GLM) was established by convolving the standard hemodynamic response function with the regressors of interest (four visual quadrants in Experiments 1 and 2; two visual hemifields in Experiment 3). Regressors of no interest (e.g., 6 head movement parameters obtained during volume registration and AFNI's baseline estimates) were also included in the GLM.

Face-selective ROIs (Experiments 1, 3 and 4) were identified for each participant using a contrast of greater activation evoked by dynamic faces than that evoked by dynamic objects, calculating significance maps of the brain using an uncorrected statistical threshold of  $p = 0.001$ . hMT+ (Experiment 2) was identified for each participant using a contrast of greater activation evoked by coherent motion than by random motion using an uncorrected statistical threshold of  $p = 0.0001$ . Within each functionally defined ROI, we then calculated the magnitude of response (percent signal change from a fixation baseline) for the visual field mapping data in each quadrant (Experiments 1 and 2) or each hemifield (Experiment 3).

### **TMS stimulation and site localization**

TMS was delivered at 60% of maximal stimulator output, using a Magstim Super

Rapid Stimulator (Magstim, UK) and a 50 mm figure-eight coil, with the coil handle pointing upwards and parallel to the midline. A single intensity was used based on previous TMS studies of the same brain areas (Pitcher et al., 2008; Pitcher, 2014). Stimuli were presented while double-pulse TMS was delivered over the target site at latencies of 60 and 100 ms after onset of the probe stimulus. These latencies were chosen to cover the most likely times of rOFA and rpSTS involvement in facial expression recognition (Pitcher, 2014).

TMS sites were individually identified in each participant using theBrainsight TMS–MRI co-registration system, utilizing individual high-resolution MRI scans for each participant. The rOFA and rpSTS were localized by overlaying individual activation maps from the fMRI localizer task onto the structural scan and the proper coil locations were marked on each participant’s head. The voxel exhibiting the peak activation in each of the functionally defined regions was used as the target.

### Experiment 1 – Responses to faces in the four quadrants of the visual field in face-selective areas

In Experiment 1, participants fixated the center of the screen while 2-sec video clips of actors performing different facial expressions were shown in the four quadrants of the visual field. To ensure that participants maintained fixation, they were required to detect the presence of an upright or inverted letter (either a T or an L) at the center of the screen. Letters (0.6° in size) were presented at fixation for 250 ms in random order and in different orientations at 4 Hz (Kastner et al., 1999). Participants were instructed

to respond when the target letter (either T or L) was shown; this occurred approximately 25% of the time. The target letter (T or L) was alternated and balanced across participants. We informed the participants that the target detection task was the aim of the experiment and we discarded any runs in which the participant scored less than seventy-five percent correct.

Visual field mapping images were acquired over 6 blocked-design functional runs lasting 408 sec each. Each functional run contained sixteen 16-sec blocks during which eight videos of eight different actors performing the same facial expression (happy, fear, disgust and neutral air-puff) were presented in one of the four quadrants of the visual field. The order was pseudo-randomized such that each quadrant appeared once every four blocks but, within each of these blocks of four, the quadrant order was randomized. After the visual field mapping blocks were completed, participants then viewed 4 blocked-design functional localizer runs lasting 234 sec each, to identify the face-selective ROIs. Finally, we collected a high-resolution anatomical scan for each participant.

#### Experiment 2 – Responses to faces in the four quadrants of the visual field in hMT+

Experiment 2 followed the same design as Experiment 1, except for the following differences. Visual field mapping images were acquired over 4 blocked-design functional runs lasting 408 sec each. After the visual field mapping blocks were completed participants viewed 2 blocked-design functional runs lasting 288 sec each, to functionally localize the motion-selective region hMT+. During the motion localizer

blocks, participants were instructed to focus on a red dot at the center of the screen.

### Experiment 3 – Responses to faces in the two hemifields of the visual field in face-selective areas

Participants fixated the center of the screen while 2-sec video clips of actors performing different facial expressions were shown in the two hemifields of the visual field. Visual field mapping images were acquired over 6 blocked-design functional runs lasting 408 sec each. Each functional run contained sixteen 16-sec blocks during which eight videos of eight different actors performing the same facial expression (happy, fear, disgust and neutral air-puff) were presented in one of the two hemifields. Eight blocks were shown in each hemifield and the order in which they appeared was randomized. After the visual field mapping blocks were completed, participants completed 6 blocked-design functional runs lasting 234 sec each to functionally localize the face-selective ROIs.

### Experiment 4 – Facial expression recognition task in the two hemifields while TMS is delivered over the rOFA and rpSTS

Double-pulse TMS was delivered over the rOFA, rpSTS and vertex while participants performed a delayed match-to-sample facial expression recognition task. The vertex condition served as a control for non-specific effects of TMS. Figure 2 displays the trial procedure. Participants sat 57 cm from the monitor with their heads stabilized in a chin rest and indicated, by a right-hand key press, whether the sample face showed the same

facial expression as the match face. During each block, facial expression stimuli were presented randomly in one of the two visual hemifields. Stimuli were presented at a size of 5 x 8 degrees of visual angle and 5 degrees of visual angle from fixation to the inside edge of the stimuli.

Participants were instructed to maintain fixation at the centre of the screen where a cross was presented during each trial. Half the trials showed picture pairs with the same expression and half showed pairs with different expressions. Identity always changed between match and sample. The six expressions were presented an equal number of times. This task has been used in previous TMS studies of facial expression recognition (Pitcher et al., 2008; Pitcher, 2014; Sliwinska & Pitcher, In Press) as well as in neuropsychological (Garrido et al., 2009; Banissy et al., 2011) and neuroimaging studies (Germine et al., 2011). Two blocks of 72 trials were presented for each TMS site (rOFA; rpSTS; vertex). Each block consisted of 36 match trials and 36 non-match trials. Site order was balanced across participants. Within each block, the trial order was randomized. Participants were instructed to respond as quickly and as accurately as possible and were not given feedback on their performance.

**Figure 2 Here.**

## TMS Experimental Procedure



**TMS protocol:** Double Pulse TMS delivered at 60 and 100ms after Target Face stimulus onset

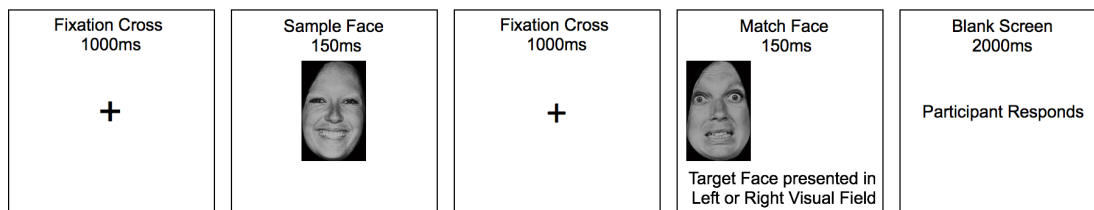


Figure 2. The timeline of the TMS experimental procedure used in Experiment 4. Participants had to judge whether the sample face and target face had the same facial expression.

### Results

#### Experiment 1 – fMRI mapping of faces in the four quadrants of the visual field in face-selective areas

Using a contrast of greater activation to faces than to objects, we identified the rFFA (mean MNI co-ordinates 43, -52, -13), IFFA (mean MNI co-ordinates -40, -54, -13), rpSTS (mean MNI co-ordinates 50, -47, 14), lpSTS (mean MNI co-ordinates -53, -51, 14) and the rOFA (mean MNI co-ordinates 41, -80, -4) in sixteen of the eighteen participants. Other face-selective ROIs were not present across all participants; the right amygdala was present in only thirteen participants, the left amygdala in eleven participants and the left OFA in seven participants. Because of this issue of reduced power, only the right FFA (rFFA), left FFA (IFFA), right pSTS (rpSTS), left pSTS (lpSTS) and rOFA were included in the subsequent ROI analysis.

Results showed that both the rFFA, IFFA and rOFA exhibited a greater response to



faces presented in the contralateral visual field than in the ipsilateral visual field. In addition, the rFFA exhibited a greater response to faces presented in the upper field than in the lower field. By contrast, the rpSTS and lpSTS exhibited no bias in response to faces presented in any of the four quadrants (see Figure 3).

**Figure 3 Here**

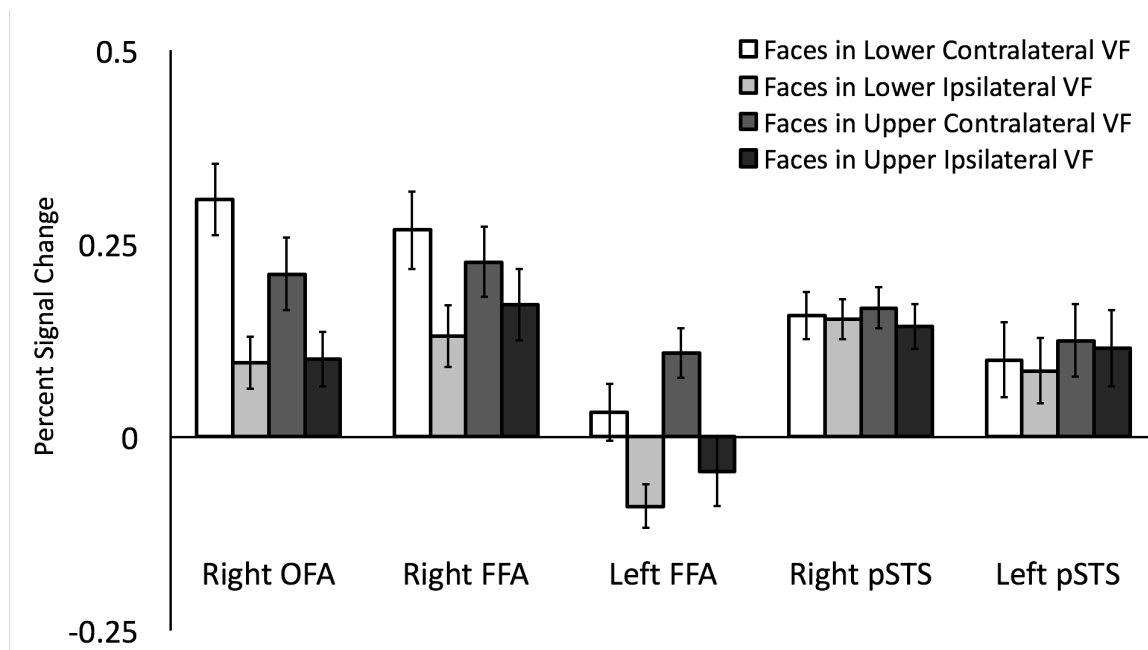


Figure 3. Percent signal change data for dynamic faces presented in the four quadrants of the visual field in face-selective regions. Results showed that the rFFA, lFFA and rOFA exhibited a significantly greater response to faces in the contralateral visual field than in the ipsilateral visual field. There were no visual field biases in the rpSTS and lpSTS. Error bars show standard errors of the mean across participants.

Percent signal change data (Figure 3) were entered into a five (ROI: rFFA, lFFA, rpSTS, lpSTS and rOFA) by two (contralateral vs. ipsilateral visual field) by two-way

(upper vs. lower visual field) repeated measures analysis of variance (ANOVA). We found main effects of ROI ( $F(4,60) = 8, p < 0.0001$ ), contralateral / ipsilateral visual field ( $F(1,15) = 10, p = 0.006$ ), and of upper / lower visual field ( $F(1,15) = 7.5, p = 0.015$ ); there was also a significant three-way interaction between ROI, contralateral vs. ipsilateral visual field and upper vs. lower visual field ( $F(4,60) = 3, p = 0.033$ ).

Separate ANOVAs were performed on each of the face-selective ROIs. The rFFA showed a significantly greater response to faces shown in the contralateral than the ipsilateral visual field ( $F(1,15) = 42, p < 0.001$ ) and to faces shown in the upper than the lower visual field ( $F(1,15) = 8, p = 0.012$ ), but there was no significant interaction between the factors ( $F(1,15) = 2.5, p = 0.15$ ). The lFFA showed the same pattern as the rFFA, with a significantly greater response to faces shown in the contralateral than the ipsilateral visual field ( $F(1,15) = 27, p < 0.001$ ) and to faces shown in the upper than the lower visual field ( $F(1,15) = 5, p = 0.04$ ), and again there was no significant interaction between the factors ( $F(1,15) = 0.8, p = 0.4$ ). The rOFA showed a significantly greater response to faces shown in the contralateral than the ipsilateral visual field ( $F(1,15) = 39, p < 0.001$ ), but there was no significant difference between faces shown in the upper and lower visual fields ( $F(1,15) = 0.2, p = 0.7$ ) nor was there a significant interaction between the factors ( $F(1,15) = 1.5, p = 0.25$ ).

By contrast, the rpSTS and lpSTS showed no significant effects of visual field. The rpSTS showed no main effect of contralateral / ipsilateral visual field ( $F(1,15) = 1, p = 0.3$ ) or of upper / lower visual field ( $F(1,15) = 2.6, p = 0.1$ ) and there was no significant interaction ( $F(1,15) = 0.1, p = 0.9$ ). The lpSTS showed no main effect of contralateral /

ipsilateral visual field ( $F(1,15) = 3, p = 0.15$ ) or of upper / lower visual field ( $F(1,15) = 3, p = 0.2$ ), and there was no significant interaction ( $F(1,15) = 0.5, p = 0.5$ ).

#### Experiment 2 – fMRI mapping of faces in the four quadrants of the visual field in hMT+

Using a contrast of activation to coherent dot motion greater than that to random dot motion, we identified the left hMT+ (mean MNI co-ordinates -43, -75, 2) and right hMT+ (mean MNI co-ordinates 42, -74, -2) in all thirteen participants. As reported by others (Watson et al., 1993; Huk et al., 2002), hMT+ was localized to the lateral occipital cortex. Results of the visual field mapping revealed that hMT+ in both hemispheres had a contralateral visual field bias but no upper or lower visual field bias (Figure 3B).

The percent signal change data were entered into a two (ROI: left vs. right HMT+) by two (contralateral vs. ipsilateral visual field) by two (upper v. lower visual field) repeated measures ANOVA. There was a significant main effect of contralateral vs. ipsilateral visual field ( $F(1,12) = 27, p < 0.0001$ ) revealing that bilateral HMT+ responded to faces in the contralateral visual field more than in the ipsilateral visual field. There was no main effect of ROI ( $F(1,12) = 0.8, p = 0.4$ ) or of upper vs. lower visual field ( $F(1,12) = 0.2, p = 0.7$ ) and no interactions approached significance ( $p > 0.15$ ).

**Figure 4 Here.**

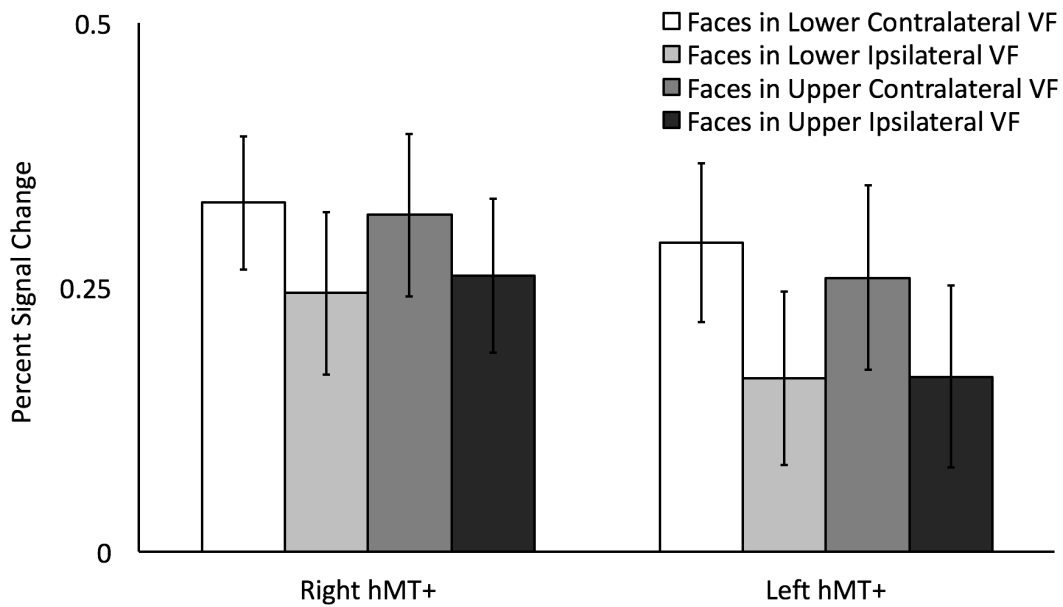


Figure 4. Percent signal change data for dynamic faces presented in the four quadrants of the visual field in left and right hMT+. Results showed that bilateral hMT+ exhibited a significantly greater response to faces in the contralateral visual field than in the ipsilateral visual field. Error bars show standard errors of the mean across participants.

### Experiment 3 – fMRI mapping of faces in the two hemifields in face-selective areas

Face-selective ROIs were identified in each participant using a contrast of activation to faces greater than that to objects. To increase the likelihood of identifying face-selective regions across both hemispheres, the number of face localizer runs was increased from four to six in Experiment 3. We identified the rFFA (mean MNI co-ordinates 42, -48, -20), rOFA (mean MNI co-ordinates 42, -78, -11), rpSTS (mean MNI co-ordinates 49, -44, 6), left FFA (lFFA) (mean MNI co-ordinates -40, -46, -22), left posterior STS (lpSTS) (mean MNI co-ordinates -53, -49, 4) and face-selective voxels in the right amygdala (mean MNI co-ordinates 23, -6, -16) in fifteen of the eighteen participants.

The left OFA was present in seven participants and the left amygdala in six participants so these areas were excluded them from further analysis.

As in Experiment 1, the rOFA, rFFA and lFFA showed a greater response to dynamic faces in the contralateral visual field than in the ipsilateral visual field. By contrast, the rpSTS, lpSTS and the right amygdala showed no visual field bias (see Figure 5).

**Figure 5 Here**

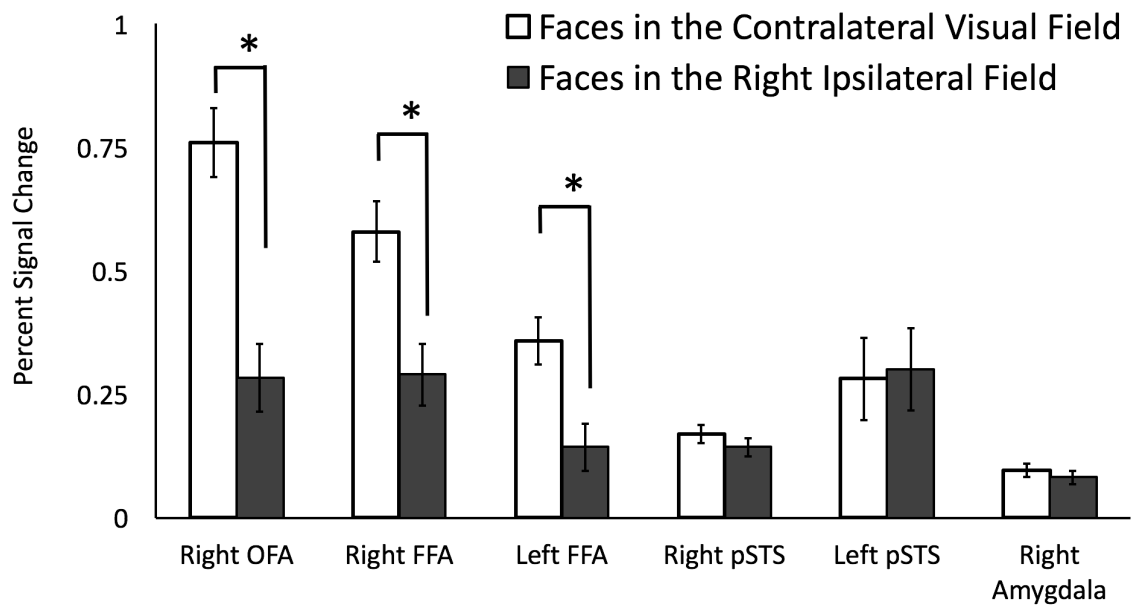


Figure 5. Percent signal change for dynamic faces presented in the contralateral and ipsilateral hemifields. Results showed that the rFFA and rOFA exhibited a significantly greater response to faces in the contralateral visual field than in the ipsilateral visual field. There were no visual field biases in the rpSTS or the right amygdala. Error bars show standard errors of the mean across participants. \* denotes a significant difference ( $p < 0.0001$ ) in post-hoc tests. Right and left FFA show the expected response of right > left. Error bars denote standard errors of the mean across participants.

Percent signal change data (Figure 5) were entered into a six (ROI: rOFA, rFFA, IFFA, rpSTS, lpSTS and right amygdala) by two (contralateral vs. ipsilateral visual field) repeated measures analysis of variance (ANOVA). Results showed significant main effects of ROI ( $F(5,70) = 4, p = 0.003$ ) and of contralateral / ipsilateral visual field ( $F(1,14) = 8, p = 0.013$ ), as well as a significant interaction of ROI and visual field ( $F(5,70) = 27, p < 0.0001$ ). Bonferroni corrected post-hoc tests showed a significantly greater response to faces in the contralateral than ipsilateral visual field in the rOFA ( $p < 0.0001$ ), rFFA ( $p < 0.0001$ ) and IFFA ( $p < 0.0001$ ) but not in the rpSTS ( $p = 0.2$ ), lpSTS ( $p = 0.8$ ) or right amygdala ( $p = 0.4$ ).

#### Experiment 4 – TMS mapping of faces in the two hemifields in the rOFA and rpSTS

In Experiment 4, TMS was delivered over the rOFA, rpSTS and the vertex while participants performed a delayed match-to-sample facial expression recognition task in each of the two visual hemifields. This was done to investigate if the differences in the visual field responses in the rOFA and rpSTS (observed in Experiments 1 and 3) is behaviorally relevant. The vertex, a point on the top of the head, acted as a control site for the non-specific effects of TMS.

Results showed that participants performed more accurately when faces were presented in the left visual field than the right visual field when TMS was delivered over the vertex (see Figure 6). This is consistent with prior results showing a left visual field advantage for behavioral face perception tasks (Sackheim et al., 1978; Young et al.,

1985). TMS delivered over the rOFA selectively disrupted task accuracy when faces were presented in the contralateral visual field but had no effect on faces presented in the ipsilateral visual field. Presumably this is because ipsilateral visual field faces were preferentially processed by face-selective areas in the left hemisphere. By contrast, TMS delivered over the rpSTS disrupted task accuracy when faces were presented in both visual fields.

Accuracy data (Figure 6) were entered into a three (ROI: rOFA, rpSTS, vertex) by two (contralateral vs. ipsilateral visual field) repeated measures ANOVA. Results showed a significant main effect of TMS site [ $F(2,26) = 8.3, p=0.002$ ] but not of visual field [ $F(1,13) = 0.6, p=0.46$ ]. Crucially, there was also a significant interaction between TMS site and visual field [ $F(2,26) = 3.9, p=0.032$ ]. To further understand what factors were driving this significant interaction we then performed two further ANOVAs that separately compared the accuracy data from the rOFA and the rpSTS to the vertex control site.

For OFA stimulation a two (TMS site: rOFA, vertex) by two (contralateral vs. ipsilateral visual field) repeated measures ANOVA showed a main effect of TMS site [ $F(1,13) = 8.1, p=0.014$ ] but not of visual field [ $F(1,13) = 0.8, p=0.82$ ]. Crucially, there was a significant interaction between TMS site and visual field [ $F(1,13) = 6.4, p=0.025$ ]. Planned Bonferroni corrections showed that TMS delivered over the rOFA impaired performance accuracy in the left visual field compared to TMS delivered over the vertex ( $p=0.016$ ). No other comparisons approached significance ( $p > 0.35$ ).

For rpSTS stimulation a two (TMS site: rpSTS, vertex) by two (contralateral vs.

ipsilateral visual field) repeated measures ANOVA showed main effects of TMS site [ $F(1,13) = 23.7, p < 0.0001$ ] and of visual field [ $F(1,13) = 7, p = 0.02$ ]. However, there was no significant interaction between TMS site and visual field [ $F(1,13) = 0.8, p = 0.8$ ]. The main effect of TMS site demonstrates that TMS delivered over the rpSTS impaired accuracy equally in both visual fields relative to vertex stimulation. The main effect of visual field is consistent with the left visual field advantage for face discrimination we observed in the vertex condition and the behavioral left visual advantage for face recognition (Sackheim et al., 1978; Young et al., 1985).

A three by two-way repeated measures ANOVA on the RT data showed no main effects of TMS site ( $p = 0.5$ ) or visual field site ( $p = 0.28$ ) and there was no significant interaction ( $p = 0.15$ ).

**Figure 6 Here.**



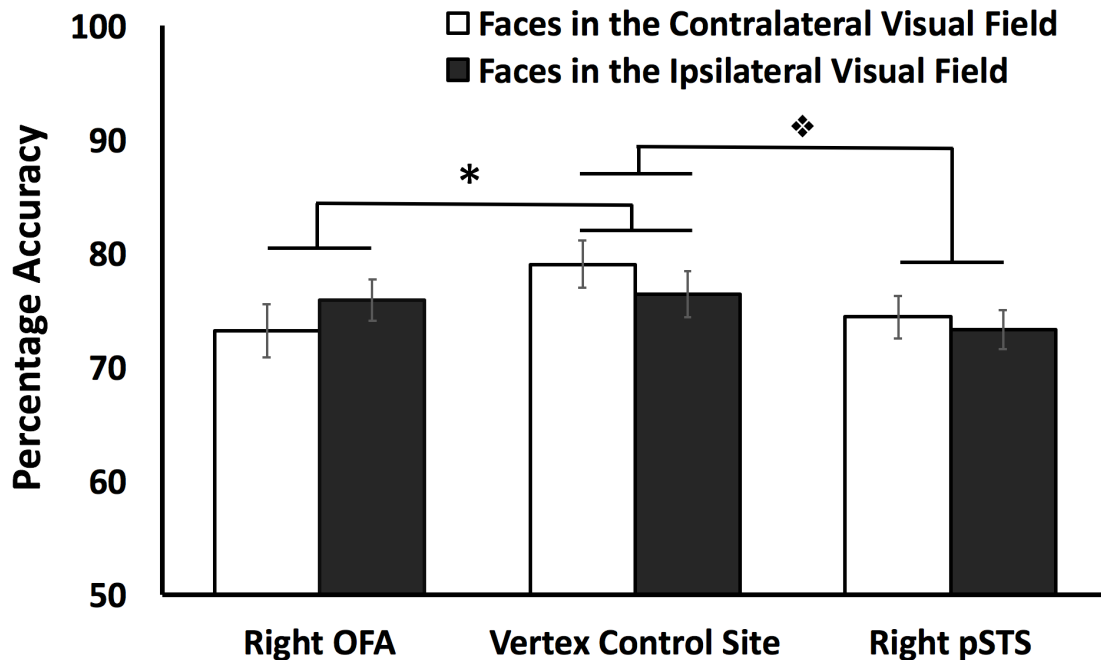


Figure. 6. Mean accuracy performance for the expression recognition task when TMS was delivered over the rOFA, rpSTS and vertex control site. Results revealed that TMS delivered over the rOFA selectively impaired task performance in the contralateral visual field only compared to vertex (\* denotes a significant interaction between TMS site and visual field,  $p=0.025$ ). By contrast TMS delivered over the rpSTS impaired task accuracy in both visual fields compared to vertex (♦ denotes a significant main effect between the rpSTS and vertex conditions,  $p < 0.0001$ ). Error bars denote standard errors of the mean across participants.

## Discussion

In the present study we investigated the neural responses to faces presented in different parts of the visual field in face-selective and motion-selective brain areas. fMRI results showed that the right fusiform face area (rFFA), left fusiform face area (lFFA) and right occipital face area (rOFA) exhibited a greater response to faces presented in the contralateral than the ipsilateral visual field, a finding consistent with prior evidence (Hemond et al., 2007, Kay et al., 2015; Silson et al., 2015). This same pattern, a greater

contralateral than ipsilateral response to face videos, was also observed in hMT+. By contrast, the face-selective region in the right and left posterior superior temporal sulcus (pSTS) did not preferentially respond to faces presented in any part of the visual field. The absence of a contralateral visual field bias for faces was also observed in face-selective voxels in the right amygdala. In a separate TMS experiment, we demonstrated that the difference in visual field responses we observed between the rpSTS and rOFA was behaviourally relevant. TMS delivered over the rpSTS disrupted performance on a facial expression recognition task in both hemifields; while TMS delivered over the rOFA disrupted facial expression recognition in the contralateral visual field only. Our results demonstrate that the contralateral visual field bias observed in the bilateral FFA, rOFA and bilateral hMT+ is absent in the bilateral pSTS.

Mapping visual field responses can reveal the functional connections between brain areas. For example, non-human primate evidence shows that the parts of visual areas V1, V2 and V4 with dense anatomical interconnections also represent the same part of the visual field (Gattass et al., 1997). A functional connection between the OFA and the FFA is consistent with both areas exhibiting a contralateral visual field bias. By contrast, if the OFA and FFA provided the sole functional input to pSTS, then the left and right pSTS would exhibit the same contralateral bias, which they did not. Our results show that there is no difference between the response to faces shown in the left and right visual field in the pSTS.

This difference in visual field response between face-selective areas ventrally (FFA and OFA) and laterally (pSTS) in the brain is also consistent with models showing that

there are two functionally distinct face pathways (Bruce & Young, 1986; Haxby et al., 2000; Calder & Young, 2005; Pitcher et al., 2011; Yovel & Duchaine, 2015). The ventral pathway, which includes the FFA, preferentially responds to invariant facial aspects, such as individual identity (Grill-Spector et al., 2004), whereas the lateral pathway, which includes the pSTS, preferentially responds to changeable facial aspects, such as emotional expression and eye-gaze direction (Hoffman & Haxby et al., 2000). The differences in visual field response we observed suggests that the interhemispheric connections between face-selective areas differs between the ventral and lateral brain surfaces. Namely, the interhemispheric connections between the bilateral pSTS are greater than those between the bilateral FFA. Future models of face perception should account for differences in the interhemispheric connections between face-selective areas.

Neuroimaging studies have shown that the pSTS exhibits a greater response to moving than to static faces (Puce et al., 1998; LaBar et al., 2002; Fox et al., 2009; Schultz & Pilz, 2009; Schultz et al., 2012 Pitcher et al., 2011; 2019), while the FFA and OFA show little, or no, preference for dynamic over static faces. This preferential response to motion indicates that the pSTS may be cortically connected to the motion-selective area hMT+ (O'Toole, 2002). An anatomical connection between motion-selective areas and the STS has been shown in both humans (Gschwind et al, 2012) and macaques (Ungerleider & Desimone, 1986; Boussaoud et al, 1990). In addition, combined TMS/fMRI and neuropsychological evidence has shown that disruption of the OFA and FFA does not impair the neural response to moving faces in the pSTS (Rezlescu et al.,

2012; Pitcher et al., 2014), suggesting that the pSTS has independent functional inputs for processing moving faces. The results of the current study indicate that a likely source of this functional input to the rpSTS are face-selective areas in the left hemisphere, perhaps most notably the lpSTS. This is consistent with a recent study showing that TMS delivered over the lpSTS impairs facial expression recognition, albeit to a lesser extent than TMS delivered over the rpSTS (Sliwiska & Pitcher, 2018).

Visual field mapping in macaques shows that visual areas that respond to motion in the contralateral visual field (MT, MST and FST) progressively represent a greater proportion of the ipsilateral visual field when moving anteriorly within the STS (Desimone & Ungerleider, 1986). This is consistent with human neuroimaging studies showing that more anterior areas of hMT+ represent a greater proportion of the ipsilateral field than more posterior areas (Huk et al., 2002; Amano et al., 2009). In our study bilateral hMT+ showed a greater response to moving faces in the contralateral than the ipsilateral visual field. This demonstrates that hMT+ cannot be the sole source of functional input into the pSTS, as at least some of the ipsilateral response we observed in the pSTS must come from the other hemisphere.

In humans, the anatomical and functional connections of the amygdala are also unclear, but non-human primate neuroanatomical studies have identified a pathway projecting down the STS into the amygdala (Aggleton et al., 1980; Stefanacci & Amaral, 2000; 2002). If a functional connection between the pSTS and amygdala exists, then the visual field responses to faces in these regions would likely be similar. In fact, we found that the right amygdala, like the rpSTS, showed no visual field bias for dynamic faces.

This similarity of the visual field responses in the rpSTS and amygdala suggests that the rpSTS could be a source of dynamic face input for the right amygdala, which is consistent with our study demonstrating that thetaburst TMS (TBS) delivered over the rpSTS reduced the fMRI response to moving faces in the right amygdala (Pitcher et al., 2017).

In sum, we investigated the visual field responses to faces in face-selective and motion-selective brain areas. Consistent with prior evidence, we observed a contralateral bias in the rFFA, lFFA and rOFA (Hemond et al., 2007, Kay et al., 2015). By contrast, we observed no such visual field bias in the rpSTS, lpSTS and face-selective voxels in the right amygdala. Our results suggest that future face perception network models should consider interhemispheric asymmetries in the functional connections of different face-selective brain areas.

### **Acknowledgements**

This work was supported by the Intramural Research Program of the National Institute of Mental Health (NCT01617408) and by grants from the Biotechnology and Biological Sciences Research Council (BB/P006981/1) and the Simons Foundation Autism Research Initiative, United States (#392150) awarded to DP. We thank Mbemba Jabbi and Nancy Kanwisher for providing stimuli. We also thank Geena Ianni, Kelsey Holiday and Magda Sliwiska for help with data collection.

## References

Aggleton JP, Burton MJ, Passingham RE. 1980. Cortical and subcortical afferents to the amygdala of the rhesus monkey (*Macaca mulatta*). *Brain Res.* 190: 347–368.

Allison T, Puce A, McCarthy G. 2000. Social perception from visual cues: role of the STS region. *Trends Cogn. Sci.* 4:267–278.

Allison T, Puce A, Spencer DD, McCarthy G. 1999. Electrophysiological studies of human face perception. I: potentials generated in occipito-temporal cortex by face and non-face stimuli. *Cereb Cortex.* 9:415-430.

Bona S, Cattaneo Z, Silvanto J. 2015. The causal role of the occipital face area (OFA) and lateral occipital (LO) cortex in symmetry perception. *Journal of Neuroscience.* 35:731-738.

Boussaoud D, Ungerleider LG, Desimone R. 1990. Pathways for motion analysis: cortical connections of the medial superior temporal and fundus of the superior temporal visual areas in the macaque. *Journal of Comp Neurol.* 296:462-95.

Bruce V, Young A. 1986. Understanding face recognition. *Br J Psychol.* 77:305-27.

Calder AJ, Young AW. 2005. Understanding the recognition of facial identity and facial

expression. *Nat Reviews Neurosci.* 6:641–651.

De Winter FL, Zhu Q, Van den Stock J, Nelissen K, Peeters R, de Gelder B, Vanduffel, W, Vandenbulcke M. 2014. Lateralization for dynamic facial expressions in human superior temporal sulcus. *NeuroImage.* 106:340–352.

Desimone R, Ungerleider LG. 1986. Multiple visual areas in the caudal superior temporal sulcus of the macaque. *Journal of Comp Neurol.* 248:164-189.

Fox CJ, Iaria G, Barton J. 2009. Defining the face-processing network: optimization of the functional localizer in fMRI. *Human Brain Mapping.* 30:1637-1651.

Gattass R, Sousa APB, Mishkin M. Ungerleider LG. 1997. Cortical projections of area V2 in the macaque. *Cereb Cortex.* 7:110-129.

Gschwind M, Pourtois G, Schwartz S, Van De Ville D, Vuilleumier P. 2012. White-Matter Connectivity between Face-Responsive Regions in the Human Brain. *Cereb Cortex.* 22:1564-1576.

Haxby JV, Hoffman EA, Gobbini MI. 2000. The distributed human neural system for face perception. *Trends Cogn Sci.* 4:223–233.

Hemond C, Kanwisher N, Op de Beeck H. 2007. A Preference for Contralateral Stimuli in Human Object- and Face-Selective Cortex. PLoS ONE. 2(6): e574.

doi:10.1371/journal.pone.0000574.

Hoffman EA, Haxby JV. 2000. Distinct representations of eye gaze and identity in the distributed human neural system for face perception. Nat Neurosci. 3:80-4.

Kanwisher N, McDermott J, Chun MM. 1997. The fusiform face area: A module in human extrastriate cortex specialised for face perception. Journal of Neuroscience. 17:4302 – 4311.

Kastner S, De Weerd P, Desimon, R, Ungerleider LG. 1999. Mechanisms of Directed Attention in the Human Extrastriate Cortex as Revealed by Functional MRI. Science. 282:108-111.

Kay KN, Weiner KS, Grill-Spector K. 2015. Attention reduces spatial uncertainty in human ventral temporal cortex ventral temporal cortex. Current Biology. 25:1-6.

Kravitz DJ, Kriegeskorte N, Baker CI. 2010. High-level visual object representations are constrained by position. Cereb Cortex. 20:2916-2925.

LaBar KS, Crupain MJ, Voyvodic JB, McCarthy G. 2003. Dynamic perception of facial



affect and identity in the human brain. *Cereb Cortex*. 13:1023-1033.

McCarthy G, Puce A, Belger A, Allison T. 1999. Electrophysiological studies of human face perception. II: response properties of face- specific potentials generated in occipitotemporal cortex. *Cereb Cortex*. 9:431-444.

Morris JS, Frith CD, Perrett DI, Rowland D, Young AW, Calder AJ, Dolan RJ. 1996. A differential neural response in the human amygdala to fearful and happy facial expressions. *Nature*. 383:812–815.

O’Toole AJ, Roark D, Abdi H. 2002. Recognition of moving faces: A psychological and neural framework. *Trends in Cognitive Sciences*. 6:261-266.

Pitcher D. 2014. Discriminating facial expressions takes longer in the posterior superior temporal sulcus than in the occipital face area. *Journal of Neuroscience*. 34:9173-9177.

Pitcher D, Dilks DD, Saxe RR, Triantafyllou C, Kanwisher N. 2011. Differential selectivity for dynamic versus static information in face selective cortical regions. *NeuroImage*. 56:2356-2363.

Pitcher D, Duchaine B, Walsh V. 2014 Combined TMS and fMRI reveals dissociable cortical pathways for dynamic and static face perception. *Current Biology*. 24:2066-

2070.

Pitcher D, Garrido L, Walsh V, Duchaine B. 2008. TMS disrupts the perception and embodiment of facial expressions. *Journal of Neuroscience*. 28:8929-8933.

Pitcher D, Ianni G, Ungerleider LG. (2019). A functional dissociation of face-, body- and scene-selective brain areas based on their response to moving and static stimuli. *Scientific Reports*.

Pitcher D, Japee S, Rauth L, Ungerleider LG. 2017. The superior temporal sulcus is causally connected to the amygdala: A combined TBS-fMRI study. *Journal of Neuroscience*. 37:1156-1161.

Pitcher D, Walsh V, Duchaine B. 2011. The role of the occipital face area in the cortical face perception network. *Experimental Brain Research*. 209:481-493.

Pitcher D, Walsh V, Yovel G, Duchaine B. 2007. TMS evidence for the involvement of the right occipital face area in early face processing. *Current Biology*. 17:1568-1573.

Puce, A., Allison, T., Bentin, S., Gore, J. C., & McCarthy, G. 1998. Temporal cortex activation in humans viewing eye and mouth movements. *J Neurosci*, 18(6), 2188-2199.

Puce A, Allison T, McCarthy G. 1999. Electrophysiological studies of human face perception. III: effects of top-down processing on face-specific potentials. *Cereb Cortex*. 9:445-458.

Rezlescu C, Pitcher D, Duchaine B. 2012. Acquired prosopagnosia with spared within-class object recognition but impaired recognition of basic-level objects. *Cognitive Neuropsychology*. 29:325-347.

Sackeim HA, Gur RC, Saucy MC. 1978. Emotions are expressed more intensely on the left side of the face. *Science*. 202:434-436.

Silson EH, Chan A, Reynolds R, Kravitz D, Baker C. 2015. A retinotopic basis for the division of high-level scene processing between lateral and ventral human occipitotemporal cortex. *Journal of Neuroscience*. 35:11921-11935.

Sliwinska MW, Pitcher D. 2018. TMS demonstrates that both right and left superior temporal sulci are important for facial expression recognition. *Neuroimage*. 183:394-400.

Stefanacci L, Amaral DG. 2000. Topographic Organization of Cortical Inputs to the Lateral Nucleus of the Macaque Monkey Amygdala: A Retrograde Tracing Study. *Journal of Comparative Neurology*. 421:52-79.

Stefanacci L, Amaral DG. 2002. Some observations on cortical inputs to the macaque monkey amygdala: An anterograde tracing study. *Journal of Comparative Neurology*. 451:301-323.

Ungerleider LG, Desimone R. 1986. Cortical connections of visual area MT in the macaque. *J Comp Neurol*. 248:190-222.

van der Gaag C, Minderaa R, Keysers C. 2007. The BOLD signal in the amygdala does not differentiate between dynamic facial expressions. *Social Cognitive and Affective Neuroscience*. 2:93-103

Watson JD, Myers R, Frackowiak RS, Hajnal JV, Woods RP, Mazziotta JC, Shipp S, Zeki S. 1993. Area V5 of the human brain: evidence from a combined study using positron emission tomography and magnetic resonance imaging. *Cereb Cortex*. 3:79–94.

Whalen PJ, Rauch SL, Etcoff NL, McInerney SC, Lee M, Jenike MA. 1998. Masked presentations of emotional facial expressions modulate amygdala activity without explicit knowledge. *Journal of Neuroscience*. 18:411-418.

Young AW, Hay DC, McWeeny KH, Ellis AW, Barry C. 1985. Familiarity decisions for faces presented to the left and right cerebral hemispheres. *Brain and Cognition*. 4:439- 450.